On Multiantenna Sensor Networks With Interference: Energy Consumption vs. Robustness

Mario Goldenbaum* and Sławomir Stańczak*†

*Lehrstuhl für Informationstheorie und theoretische Informationstechnik, Technische Universität Berlin, Einsteinufer 25, 10587 Berlin, Germany

†Fraunhofer Institute for Telecommunications, Heinrich-Hetz-Institute, Einsteinufer 37, 10587 Berlin, Germany

***Abstract*—In this paper, we consider power-controlled wireless multiantenna sensor networks with interference and study the general trade-off between energy consumption and quality-of-service expressed in terms of the signal-to-interference ratio (SIR). First, we develop a model for the energy consumption of multiantenna nodes (i.e., energy consumption for transmission and hardware) and then study the trade-off between accuracy and energy costs for channel estimation by deriving a bound for the estimation error variance, since most multiantenna strategies require adequate channel knowledge. Then, we numerically compare different MIMO strategies with the energy consumption and the achievable SIR of a standard SISO system, to obtain insights into the strength of the discussed trade-off and to provide guidelines on the choice of strategies for different applications.**

I. Introduction

Some of the most exciting applications for wireless sensor networks require that sensor nodes be powered by batteries. Energy efficiency is therefore a major design paradigm to ensure a long network lifetime. In addition to the scarce energy resources, the challenge is exacerbated by wireless sensor applications that often involve performing certain tasks having significantly different (more stringent) requirements with respect to data rate, delay and reliability than applications in traditional wireless networks. An example of such an application is fire detection where the task to perform is a fast and reliable detection of a fire based on some noisy sensor measurements. For this application, robust communication with very low delay is of highest priority during alarm situations, which can be achieved at the cost of higher energy consumption per transmitted bit due to a general trade-off between energy consumption and quality of service (QoS).

From information theory it is well known that multiple-input multiple-output (MIMO) systems offer higher robustness against link failures (or higher data rates) by the same transmit power budget than single-input single-output (SISO) counterparts [1]. That is why MIMO systems are highly attractive for sensor network applications with strict QoS-requirements. The information-theoretic insights, however, ignore the increase in *hardware/circuit energy consumption* due to additional components (e.g., mixer, DA-converters, filters, amplifiers, microcontrollers), which in the case of wireless sensor applications is often comparable to the transmit energy consumption [2]. Focusing on minimizing transmission energies only is therefore highly insufficient, especially because the majority of MIMO strategies require appropriate channel state information (CSI) at the transmitter and/or receiver side, typically acquired by transmitting pilots, which further increases the total energy consumption.

In this paper, we study the trade-off between energy consumption and robustness in uncoordinated power-controlled sensor networks, consisting of simultaneously transmitting multiantenna sensor nodes, where the robustness is measured in terms of achievable signal-to-interference ratios (SIRs). First we develop a model for the energy consumption of multiantenna nodes (i.e., transmission energy plus hardware energy), and then we study the trade-off between accuracy and energy costs for standard least squares training-based channel estimation by deriving a bound for the estimation error variance that depends on the length of pilot-sequences, the number of interfering nodes, the worst-case interference power, etc. It is clear that channel estimation errors result in increased overall receiver noise powers and thus in decreased SIR values. Therefore, to increase SIRs, the length of pilot-sequences has to be increased, which in turn increases the energy consumption for channel estimation. The impact of this trade-off on the performance of different MIMO transmit and receive strategies is then explored by numerical examples.

A. Related Work

To the best of our knowledge, Cui et al. were the first who analyzed in [2] whether multiantenna nodes are useful for sensor network applications at all due to the increase in circuit energy consumption proportional to the number of antennas. In contrast to the single-user system model in [3], Feistel et al. considered in [4] the minimization of the overall energy consumption in a network of interfering MIMO links by determining the optimal number of parallel data streams per link. Using the same system model, Wiczanowski et al. characterized in [5] different regimes of transmit covariance matrices that allow to better understand the behavior and the design of energy efficient MIMO strategies. More recently Chong and Jorswieck provided in [3] an energy-efficient power

The research in this paper was supported by the German Research Foundation (DFG) under grant STA 864/3-1 and by the Federal Ministry of Economics and Technology (BMWi), Germany, under grant 01ME11024.

978-1-4577-1924-0/12/$26.00 ©2012 IEEE

control mechanism for a single-user MIMO link (i.e., the interference-free downlink in a cellular system) that suffers from fading by also taking the hardware energy consumption into account.

B. Paper Organization

The rest of the paper is organized as follows. In Section II we present our interference network model as well as the model for the energy consumption of multiantenna sensor nodes. Section III takes a closer look at the impact of channel estimation errors on achievable SIRs, while we numerically compare in Section IV different multiantenna strategies with a SISO system regarding the achievable robustness and energy consumption. Finally, Section V concludes the paper.

C. Notational Remarks

Vectors and matrices are denoted by bold lowercase and bold uppercase letters, respectively. The conjugate, the transpose and the Hermitian transpose of a vector or a matrix are denoted by $(\cdot)^*$, $(\cdot)^{\mathsf{T}}$ and $(\cdot)^{\mathsf{H}}$, while $\mathrm{tr}\{\boldsymbol{A}\}$, $\rho(\boldsymbol{A})$ and $\|\boldsymbol{A}\|_F$ are the trace, the spectral radius and the Frobenius norm of matrix $\boldsymbol{A}$.

II. System Model

A. Network Model

Consider a power-controlled wireless sensor network of fixed topology that consists of $K \in \mathbb{N}$ spatially distributed and simultaneously active transmitter-receiver pairs (i.e., single-hop links), represented by the set $\mathcal{K} := \{1, \ldots, K\}$. All transmitters and receivers are identical and equipped with $N \in \mathbb{N}$ antenna elements. The frequency-flat baseband channel between the transmitter of link $\ell \in \mathcal{K}$ and the receiver of link $k \in \mathcal{K}$ is described by the random but fixed matrix $\boldsymbol{H}^{(k,\ell)} = (h_{ij}^{(k,\ell)}) \in \mathbb{C}^{N \times N}$ such that the complex vector-valued symbol received at the receiver of the k^{th} MIMO link can be written as

$$\boldsymbol{y}^{(k)} = \boldsymbol{H}^{(k,k)}\boldsymbol{x}^{(k)} + \sum_{\ell \neq k} \boldsymbol{H}^{(k,\ell)}\boldsymbol{x}^{(\ell)} + \boldsymbol{n}^{(k)} \tag{1}$$

with $\boldsymbol{x}^{(k)} \in \mathbb{C}^N$ being the transmit vector of link k, $k \in \mathcal{K}$. The corresponding receiver noise is described by $\boldsymbol{n}^{(k)} \in \mathbb{C}^N$, where we assume $\mathbb{E}\{\boldsymbol{n}^{(k)}\} = \boldsymbol{0}$ and $\mathbb{E}\{\boldsymbol{n}^{(k)}\boldsymbol{n}^{(k)\mathsf{H}}\} = \sigma_k^2 \boldsymbol{I}_N$, for all $k \in \mathcal{K}$, with $\sigma_k^2 > 0$ the noise variance. Furthermore, the channels, the transmit signals and the noise are mutually independent.

Let $\boldsymbol{p} := [p_1, \ldots, p_K]^{\mathsf{T}} \in \mathcal{P}$ be the vector of transmit powers $p_k = \mathbb{E}\{\|\boldsymbol{x}^{(k)}\|_2^2\}$, $k \in \mathcal{K}$, and let $\mathcal{P} := \{\boldsymbol{p} \in \mathbb{R}_+^K \,|\, \forall k \in \mathcal{K} : p_k \leq P\}$ be the set of feasible power vectors, respectively, where $P > 0$ denotes a common power constraint. Then, the SIR on link $k \in \mathcal{K}$ has the form

$$\mathrm{SIR}_k(\boldsymbol{p}) := \frac{p_k}{I_k(\boldsymbol{p})} \;, \tag{2}$$

with $I_k : \mathcal{P} \to \mathbb{R}_{++}$ the affine interference function [6]

$$I_k(\boldsymbol{p}) = (\boldsymbol{V}\boldsymbol{p} + \boldsymbol{z})_k = \sum_{\ell \in \mathcal{K}} v_{k\ell} p_\ell + z_k \;. \tag{3}$$

Here, the nonnegative gain matrix $\boldsymbol{V} = (v_{k\ell}) \in \mathbb{R}_+^{K \times K}$ encompasses the effective power gains $v_{k\ell} := \frac{V_{k\ell}}{V_k} \geq 0$, with $v_{kk} = 0$ (i.e., no self-interference), where $V_k > 0$ denotes the signal path power gain and $V_{k\ell}$ the power gain of the interference path from the ℓ^{th} transmitter to the k^{th} receiver, respectively. Finally,

$$\boldsymbol{z} = [z_1, \ldots, z_K]^{\mathsf{T}} = \left[\frac{\sigma_1^2}{V_1}, \ldots, \frac{\sigma_K^2}{V_K}\right]^{\mathsf{T}} \in \mathbb{R}_{++}^K \tag{4}$$

is the vector of effective noise variances.

Remark 1. Note that in general, the effective power gains $v_{k\ell}$ and the effective noise variances z_k depend on channel realizations as well as on concrete adaptive transmit and receive strategies (e.g., on transmit and receive beamformers), which can be seen in Section IV-A.

In this paper, the SIR (2) is a QoS measure of interest in the sense that larger SIR values imply a better QoS performance and we call a transceiver strategy more *robust* against link failures compared to other strategies, if it is possible to achieve larger SIR targets at the same power constraint. In what follows, let $\gamma > 0$ be any common SIR target, which means that

$$\forall k \in \mathcal{K} : \mathrm{SIR}_k(\boldsymbol{p}) \geq \gamma \tag{5}$$

is desired.[1] Solving this linear system of inequalities leads to the optimal transmit power vector/allocation

$$\boldsymbol{p}^\star(\gamma) = \left(\frac{1}{\gamma}\boldsymbol{I}_K - \boldsymbol{V}\right)^{-1} \boldsymbol{z} \;, \tag{6}$$

fulfilling the SIR target with equality on each link, such that $p_k^\star(\gamma)$ is the necessary transmit power consumption of link $k \in \mathcal{K}$.

Remark 2. Since the gain matrix $\boldsymbol{V}$ in (3) is nonnegative and the corresponding vector $\boldsymbol{z}$ of effective noise variances strictly positive, the solution (6) exists, is unique and strictly positive if and only if $\rho(\boldsymbol{V}) < \frac{1}{\gamma}$ [6, Theorem A.51]. Of course, the existence does not necessarily imply $\boldsymbol{p}^\star(\gamma) \in \mathcal{P}$.

B. Hardware and Energy Model

The energy consumption of a particular link crucially depends on the following:

1) Application
2) Protocols (generally specified by a standard)
3) Baseband signal processing including MIMO transmit and receive strategies
4) Hardware realization including RF components

For example, regarding the network model from Section II-A, the sensor network application defines the SIR target γ (i.e., the required robustness) and thus the necessary transmit power budget (6). Therefore, we present in this section an energy model that takes 1)–4) into account. To this end, we first introduce an appropriate frame model.

[1] Only for ease of presentation, we use in this paper a common SIR target γ on each link. A generalization to individual SIR targets $\gamma_k > 0$, $k = 1, \ldots, K$, is straightforward.

1) Frame Model: Sensor node design generally follows the low duty cycle principle, which means that a node is asleep/passive for the major part of a frame, wakes up shortly for processing and transmitting data and returns to sleep. Therefore, we consider in this paper the following frame model

$$T_\text{F} := T_\text{a} + T_\text{b} + T_\text{c} + T_\text{d} \tag{7}$$

with temporal contributions

- T_F: the frame length in seconds
- T_a: the fraction of T_F for transmitting channel estimation pilots
- T_b: the fraction of T_F for channel estimation computations in the microcontroller
- T_c: the fraction of T_F for payload transmission
- T_d: the fraction of T_F in which the transmitter *and* the receiver of a link are in their passive modes.

Let $L \in \mathbb{N}$ be the length of complex-valued pilot sequences and let $R \in \mathbb{R}_+$ be the data rate. Then, the time per frame required for channel estimation purposes can be modeled as

$$T_\text{a} = L/R\,. \tag{8}$$

After receiving pilots, the channel estimate is computed in the microcontroller and the corresponding computation time mainly depends on the number of required arithmetic operations. The time for a single arithmetic operation is usually specified as a multiple $n_\text{cycles} \in \mathbb{N}$ of main clock cycles [7] so that we model T_b as

$$T_\text{b} = T'_\text{b} + T_0 := (1+\beta)T'_\text{b} = (1+\beta)n\frac{n_\text{cycles}}{f_\text{MCLK}}\,. \tag{9}$$

Here, $f_\text{MCLK} \in \mathbb{R}_{++}$ denotes the main clock frequency of the microcontroller and $n \in \mathbb{N}$ the number of arithmetic operations required to compute the channel estimate. The term T'_b describes the computation effort and $T_0 := \beta T'_\text{b}$, $\beta \in \mathbb{R}_{++}$, corresponding temporal contributions generated by read/write operations, loops for addressing, copying coefficients into operand registers, etc.

Now, let $B \in \mathbb{N}$ be a fixed number of complex-valued payload symbols that have to be transmitted in each frame. Then, the time per frame for payload transmission is

$$T_\text{c} = B/R\,. \tag{10}$$

With (8), (9) and (10), the time per frame in which the transmitter and the receiver of a link are in its passive modes is

$$T_\text{d} = T_F - (T_\text{a} + T_\text{b} + T_\text{c})\,. \tag{11}$$

2) Energy Model: According to the frame model (7), the energy consumption per frame is modeled as

$$E_\text{F} := E_\text{a} + E_\text{b} + E_\text{c} + E_\text{d}\,. \tag{12}$$

Most existing single-antenna sensor node hardware is based on an integrated design in which the energy consumption is mainly determined by the microcontroller and the transceiver-chip [8]. In order to enable the modeling of the energy summands in (12), we assume that a multiantenna node is built of a bank of low-power transceiver chips (i.e., one for each antenna).

TABLE I
POWER CONSUMPTIONS OF THE MICROCONTROLLER (μC) AND THE TRANSCEIVER-CHIP IN THEIR PASSIVE AND ACTIVE MODES.

P^p_mc	power consumption of the μC in its passive mode
P^a_mc	basic power consumption of the μC in its active mode
P^r_tc	power consumption of the transceiver-chip in its receive mode
P^p_tc	power consumption of the transceiver-chip in one of its passive modes $P^{\text{p}_\text{s}}_\text{tc}$, $P^{\text{p}_\text{i}}_\text{tc}$
$P^{\text{p}_\text{s}}_\text{tc}$	power consumption of the transceiver-chip in its passive "sleep" mode in which most parts of the transceiver are switched off
$P^{\text{p}_\text{i}}_\text{tc}$	power consumption of the transceiver-chip in its passive "idle" mode in which the transceiver is sensing the wireless medium for a receive signal
P^ce_in	input power consumption of the transceiver-chip when sending pilot sequences for channel estimation

To maintain long battery lifetimes, available low-power devices offer multiple active and passive modes in which different hardware components are switched on/off. Table I summarizes the corresponding elements that are used in the following to meaningfully model the summands in (12).

The energy consumption per frame while transmitting channel estimation pilots is modeled as

$$E_\text{a} = \xi T_\text{a}\big(NP^\text{ce}_\text{in} + NP^\text{r}_\text{tc} + 2P^\text{a}_\text{mc}\big)\,, \tag{13}$$

where $\xi = 1$ if the considered MIMO strategy requires channel knowledge at the receiver and $\xi = 2$ if the strategy requires channel knowledge at both sides of the link, respectively. Let $f : \mathbb{R}_+ \to \mathbb{R}_+$ be a bijective mapping that appropriately approximates the loss characteristic of the transceiver-chip in its transmission mode[2]. In other words, f specifies the input power that is necessary to provide a desired transmit power on a certain link such that the input power for transmitting pilots (uniformly distributed over transmit antennas) is $P^\text{ce}_\text{in} = \frac{1}{N}f(p_k)$, $p_k \in [0, P]$, $k \in \mathcal{K}$.

The energy consumption per frame for channel estimation computations in the micro controller is modeled as

$$E_\text{b} = T_\text{b}\big(\xi P^\text{a}_\text{mc} + (2-\xi)P^\text{p}_\text{mc} + 2NP^\text{p}_\text{tc}\big)\,, \tag{14}$$

$P^\text{p}_\text{tc} \in \{P^{\text{p}_\text{s}}_\text{tc}, P^{\text{p}_\text{i}}_\text{tc}\}$, with $\xi \in \{1,2\}$ as before. We assume that while computing the estimate, the transceiver chips at both sides of the link and at each antenna are in its passive modes, resulting in the term $2NP^\text{p}_\text{tc}$.

With (10), the energy expenditure for transmitting B bits per frame is modeled as

$$E_\text{c} = T_\text{c}\big(\|\boldsymbol{p}^\star_\text{in}(\gamma)\|_1 + NP^\text{r}_\text{tc} + 2P^\text{a}_\text{mc}\big)\,, \tag{15}$$

where $\boldsymbol{p}^\star_\text{in}(\gamma) = [p^\star_{\text{in},1}(\gamma), \ldots, p^\star_{\text{in},K}(\gamma)]^\mathsf{T} \in \mathbb{R}^K_+$ denotes the vector of input powers that are necessary to

[2]The measured loss characteristic of a particular transceiver chip is usually depicted in its datasheet.

support the optimal transmit powers (6) (i.e., $\boldsymbol{p}^\star(\gamma) = \left[f^{-1}(p^\star_{\text{in},1}(\gamma)),\ldots,f^{-1}(p^\star_{\text{in},K}(\gamma))\right]^\mathsf{T}$).

Since T_d is the time per frame in which the transmitter and the receiver of a link are in its passive mode, we model the corresponding energy consumption as

$$E_\text{d} = T_\text{d}\big(2P^\text{p}_\text{mc} + 2NP^\text{p}_\text{tc}\big)\ , \tag{16}$$

$P^\text{p}_\text{tc} \in \{P^{\text{p}_\text{s}}_\text{tc}, P^{\text{p}_\text{i}}_\text{tc}\}$ (see Table I).

III. Channel Estimation

A. Linear Least Squares

To incorporate the SIR deterioration due to channel estimation errors, we model the channel matrix of link $k \in \mathcal{K}$ as

$$\boldsymbol{H}^{(k,k)} = \hat{\boldsymbol{H}}^{(k,k)}_\text{LS} + \boldsymbol{\Delta}^{(k,k)}_{\boldsymbol{H}}\ , \tag{17}$$

where $\hat{\boldsymbol{H}}^{(k,k)} \in \mathbb{C}^{N\times N}$ denotes the linear least squares (LS) estimate of $\boldsymbol{H}^{(k,k)}$ and $\boldsymbol{\Delta}^{(k,k)}_{\boldsymbol{H}} \in \mathbb{C}^{N\times N}$ is the corresponding estimation error. Hence, it follows immediately from (1)

$$\begin{aligned}\boldsymbol{y}^{(k)} &= \left(\hat{\boldsymbol{H}}^{(k,k)} + \boldsymbol{\Delta}^{(k,k)}_{\boldsymbol{H}}\right)\boldsymbol{x}^{(k)} + \sum_{\ell\neq k}\boldsymbol{H}^{(k,\ell)}\boldsymbol{x}^{(\ell)} + \boldsymbol{n}^{(k)} \\ &= \hat{\boldsymbol{H}}^{(k,k)}\boldsymbol{x}^{(k)} + \tilde{\boldsymbol{n}}^{(k)}\end{aligned} \tag{18}$$

with $\tilde{\boldsymbol{n}}^{(k)} := \boldsymbol{\Delta}^{(k,k)}_{\boldsymbol{H}}\boldsymbol{x}^{(k)} + \sum_{\ell\neq k}\boldsymbol{H}^{(k,\ell)}\boldsymbol{x}^{(\ell)} + \boldsymbol{n}^{(k)} \in \mathbb{C}^N$ being the overall noise.[3] Let us assume that $\forall k,\ell$: $\mathbb{E}\{\boldsymbol{H}^{(k,\ell)}\} = \boldsymbol{0}$ and that all $\boldsymbol{H}^{(k,\ell)}$ are spatially white (i.e., $\mathbb{E}\{\boldsymbol{H}^{(k,\ell)\mathsf{H}}\boldsymbol{H}^{(k,\ell)}\} = N\big(\sigma^{(k,\ell)}_{\boldsymbol{H}}\big)^2\boldsymbol{I}_N$, $\big(\sigma^{(k,\ell)}_{\boldsymbol{H}}\big)^2 > 0$, for all k,ℓ) as well as mutually independent. Then, it follows $\mathbb{E}\{\boldsymbol{\Delta_H}^{(k,k)}\boldsymbol{\Delta_H}^{(k,k)\mathsf{H}}\} = N\big(\sigma^{(k,k)}_{\boldsymbol{\Delta_H}}\big)^2\boldsymbol{I}_N$, with $\big(\sigma^{(k,k)}_{\boldsymbol{\Delta_H}}\big)^2 \geq 0$ being the estimation error variance, and

$$\begin{aligned}\mathbb{E}\{\tilde{\boldsymbol{n}}^{(k)}\tilde{\boldsymbol{n}}^{(k)\mathsf{H}}\} &= \sum_{\ell\neq k}\mathbb{E}\{\boldsymbol{H}^{(k,\ell)}\boldsymbol{x}^{(\ell)}\boldsymbol{x}^{(\ell)\mathsf{H}}\boldsymbol{H}^{(k,\ell)\mathsf{H}}\} \\ &\quad + \left(\big(\sigma^{(k,k)}_{\boldsymbol{\Delta_H}}\big)^2 p_k + \sigma_k^2\right)\boldsymbol{I}_N\end{aligned} \tag{19}$$

the covariance matrix of the overall noise. The second row in (19) indicates that the channel estimation error results in an increased noise variance as long as the estimation error variance is different from zero. Therefore, we define

$$\tilde{\sigma}_k^2 := (\sigma^{(k,k)}_{\boldsymbol{\Delta_H}})^2 p_k + \sigma_k^2 \leq (\sigma^{(k,k)}_{\boldsymbol{\Delta_H}})^2 P + \sigma_k^2 \tag{20}$$

to be the overall noise variance.

To find a simple and tractable parametrization of $\big(\sigma^{(k,k)}_{\boldsymbol{\Delta_H}}\big)^2$, we assume now that the transmitter of link $k \in \mathcal{K}$ transmits pilot sequences of length $L \in \mathbb{N}$ per antenna, $L \geq N$. Grouping the corresponding L receive vectors into a matrix of dimension $N \times L$, (1) yields

$$\boldsymbol{Y}^{(k)} = \boldsymbol{H}^{(k,k)}\boldsymbol{S}^{(k)} + \underbrace{\sum_{\ell\neq k}\boldsymbol{H}^{(k,\ell)}\boldsymbol{X}^{(\ell)} + \boldsymbol{N}^{(k)}}_{=:\tilde{\boldsymbol{N}}^{(k)}\in\mathbb{C}^{N\times L}} \tag{21}$$

[3]Even if, for example, linear minimum mean-square-error (MMSE) estimation generally leads to a better estimation performance, we assume LS estimation in this paper due to its lower complexity and due to the fact that MMSE estimators generally require knowledge about the covariance matrix of the overall noise $\tilde{\boldsymbol{n}}^{(k)}$, $k \in \mathcal{K}$.

with $\boldsymbol{X}^{(\ell)} \in \mathbb{C}^{N\times L}$, $\ell \in \mathcal{K}\backslash\{k\}$, the independent interfering transmit signals and $\boldsymbol{S}^{(k)} \in \mathbb{C}^{N\times L}$ the pilot symbol matrix that is known to the receiver of link $k \in \mathcal{K}$. Due to the transmit power constraint, $\text{tr}\{\boldsymbol{S}^{(k)}\boldsymbol{S}^{(k)\mathsf{H}}\} = Lf^{-1}(P^\text{ce}_\text{in}) \leq LP$ has to be fulfilled, for all $k \in \mathcal{K}$. Using the received training block (21), the LS estimate of $\boldsymbol{H}^{(k,k)}$ has the explicit form [9]

$$\hat{\boldsymbol{H}}^{(k,k)}_\text{LS} = \boldsymbol{Y}^{(k)}\boldsymbol{S}^{(k)\mathsf{H}}\big(\boldsymbol{S}^{(k)}\boldsymbol{S}^{(k)\mathsf{H}}\big)^{-1} = \boldsymbol{Y}^{(k)}\boldsymbol{S}^{(k)\dagger}\ , \tag{22}$$

such that the estimation error variance can be expressed as

$$\begin{aligned}\big(\sigma^{(k,k)}_{\boldsymbol{\Delta_H}}\big)^2 &= \frac{1}{N^2}\mathbb{E}\left\{\big\|\boldsymbol{\Delta_H}^{(k,k)}\big\|_F^2\right\} \\ &= \frac{1}{N^2}\,\text{tr}\left\{(\boldsymbol{S}^{(k)\dagger})^\mathsf{H}\mathbb{E}\{\tilde{\boldsymbol{N}}^{(k)\mathsf{H}}\tilde{\boldsymbol{N}}^{(k)}\}\boldsymbol{S}^{(k)\dagger}\right\}.\end{aligned} \tag{23}$$

Under the previous assumptions and the assumption that the interfering transmit symbols are uncorrelated, the expected value in the second row of (23) is

$$\begin{aligned}\mathbb{E}\{\tilde{\boldsymbol{N}}^{(k)\mathsf{H}}\tilde{\boldsymbol{N}}^{(k)}\} &= \sum_{\ell\neq k}\mathbb{E}\left\{\boldsymbol{X}^{(\ell)\mathsf{H}}\boldsymbol{H}^{(k,\ell)\mathsf{H}}\boldsymbol{H}^{(k,\ell)}\boldsymbol{X}^{(\ell)}\right\} \\ &\quad + N\sigma_k^2\boldsymbol{I}_L \\ &= \Big(N\sum_{\ell\neq K}\big(\sigma^{(k,\ell)}_{\boldsymbol{H}}\big)^2 p_\ell + N\sigma_k^2\Big)\boldsymbol{I}_L\ .\end{aligned} \tag{24}$$

Now, combining $(\sigma^{(k)}_{\tilde{\boldsymbol{N}}})^2 := N\sum_{\ell\neq K}\big(\sigma^{(k,\ell)}_{\boldsymbol{H}}\big)^2 p_\ell + N\sigma_k^2$ with (23) results in

$$\big(\sigma^{(k,k)}_{\boldsymbol{\Delta_H}}\big)^2 = \frac{(\sigma^{(k)}_{\tilde{\boldsymbol{N}}})^2}{N^2}\,\text{tr}\left\{\big(\boldsymbol{S}^{(k)}\boldsymbol{S}^{(k)\mathsf{H}}\big)^{-1}\right\}\ . \tag{25}$$

The following Lemma provides a lower bound for the trace.

Lemma 1. Let the Hermitian matrix $\boldsymbol{S}^{(k)}\boldsymbol{S}^{(k)\mathsf{H}} \in \mathbb{C}^{N\times N}$ be invertible. Then,

$$\text{tr}\Big\{\big(\boldsymbol{S}^{(k)}\boldsymbol{S}^{(k)\mathsf{H}}\big)^{-1}\Big\} \geq \frac{N^2}{\text{tr}\big\{\boldsymbol{S}^{(k)}\boldsymbol{S}^{(k)\mathsf{H}}\big\}}\ , \tag{26}$$

with equality if and only if $\boldsymbol{S}^{(k)}\boldsymbol{S}^{(k)\mathsf{H}} = \alpha\boldsymbol{I}_N$, for some constant $\alpha \in \mathbb{R}$.

Proof: The proof can be found in [10]. ∎

Proposition 1. Let the channels in (1) be spatially white with variances $\big(\sigma^{(k,\ell)}_{\boldsymbol{H}}\big)^2 > 0$, $k,\ell \in \mathcal{K}$, let the transmitter of link $k \in \mathcal{K}$ transmit pilot sequences at the maximum transmit power (i.e., $\text{tr}\{\boldsymbol{S}^{(k)}\boldsymbol{S}^{(k)\mathsf{H}}\} = LP$), and let all interferers transmit data with maximum transmit powers as well. Then, under this worst-case interference power assumption, the estimation error variance can be lower bounded by

$$\big(\sigma^{(k,k)}_{\boldsymbol{\Delta_H}}\big)^2 \geq \frac{NP\sum_{\ell\neq k}\big(\sigma^{(k,\ell)}_{\boldsymbol{H}}\big)^2 + N\sigma_k^2}{LP}\ , \tag{27}$$

with equality if and only if orthogonal pilot-sequences are used.

Remark 3. Note that (27) depends on the number of interferers, because $\sum_{\ell\neq k}\big(\sigma^{(k,\ell)}_{\boldsymbol{H}}\big)^2$ in the numerator consists of $K-1$ nonzero elements.

According to Proposition 1, any training matrix that satisfies

$$\boldsymbol{S}^{(k)}\boldsymbol{S}^{(k)\mathsf{H}} = \frac{LP}{N}\boldsymbol{I}_N \tag{28}$$

minimizes the estimation error variance, such that (22) reduces to

$$\hat{\boldsymbol{H}}_{\text{LS}}^{(k,k)} = \frac{N}{LP}\boldsymbol{Y}^{(k)}\boldsymbol{S}^{(k)\mathsf{H}} \; . \tag{29}$$

Remark 4. In the case of colored interference, the covariance structure of the interference crucially impacts the design of pilot sequences, such that (28) is generally suboptimal [11].

Assuming orthogonal pilot sequences, $N, K < \infty$ and using (27) in (20), we conclude that $\forall k \in \mathcal{K} : \lim_{L\to\infty} \tilde{\sigma}_k^2 = \sigma_k^2$ as one would expect for an adequate channel estimator. Replacing the noise variances in (4) by $\tilde{\sigma}_1^2, \ldots, \tilde{\sigma}_K^2$ provides the desired trade-off between achievable SIR performance and energy consumption since the channel estimation errors increase the interference and thus decrease the SIR. To improve the performance, the length of pilot sequences has to be increased at the expense of a higher energy consumption.

Corollary 1. Let $\varepsilon > 0$ be any desired estimation accuracy on link $k \in \mathcal{K}$ with respect to $\big(\sigma_{\boldsymbol{\Delta_H}}^{(k,k)}\big)^2$ and let $\boldsymbol{S}^{(k)}$ such that (28) is satisfied. Then, a sufficient condition for achieving $\big(\sigma_{\boldsymbol{\Delta_H}}^{(k,k)}\big)^2 \leq \varepsilon$ is

$$L \geq \frac{NP\sum_{\ell\neq k}\big(\sigma_{\boldsymbol{H}}^{(k,\ell)}\big)^2 + N\sigma_k^2}{\varepsilon P} \; . \tag{30}$$

B. Comments on Energy Consumption

To efficiently perform computations on a sensor node, the most suitable microcontrollers have a hardware multiplier that rapidly performs multiply-accumulate operations [12]. Since a standard matrix multiplication merely consists of additions and multiplications, the least squares estimator (29) requires $n' = N^2L$ complex-valued multiply-accumulate operations. Multiplying two complex numbers in the most naive way, however, requires 4 real additions and 4 real multiplications so that we assume in the following that the time required to perform complex-valued multiply-accumulate operations is higher by a factor of 4. Hence, (9) has with $n = 4n' = 4N^2L$ the form

$$T_\text{b}' = 4N^2L\frac{n_\text{cycles}}{f_\text{MCLK}} \; . \tag{31}$$

Remark 5. An appropriate determination of the number n_cycles of cycles per multiply-accumulate operation is generally difficult since n_cycles depends on the program code, the chosen compiler and the used programming language. Assuming an ideal implementation of the least squares estimator in machine language, we choose $n_\text{cycles} = 3$ for the numerical examples in Section IV [7].

Remark 6. Instead of modeling the energy consumption for computation purposes such as in (14) and (9), a more precise model could be

$$E_\text{b} = n_\text{a}E_\text{add} + n_\text{m}E_\text{mult} + E_0 \; , \tag{32}$$

where $n_\text{a}, n_\text{m} \in \mathbb{N}$ denote the numbers of required real floating-point additions and multiplications, $E_\text{add}, E_\text{mult} \in \mathbb{R}_+$ the corresponding energy consumptions for a single floating-point addition or multiplication and $E_0 \in \mathbb{R}_+$ summarizes the energy consumption for certain overhead (e.g., reading from memory, copying coefficients), respectively. Following the complexity analysis for least squares channel estimation in [13] leads to

$$n_\text{a} = \left(\frac{35}{2}N^2 - \frac{7}{2}N\right)L + \frac{7}{6}N^3 - 3N^2 - \frac{13}{6}N \tag{33}$$

$$n_\text{m} = \left(\frac{15}{2}N^2 + \frac{5}{2}N\right)L + \frac{1}{2}N^3 + N^2 + \frac{1}{2}N \tag{34}$$

required real floating-point multiplications and additions to perform (22). In the case of white interference, (33) and (34) reduce to

$$n_\text{a} = 3N^2L \tag{35}$$

$$n_\text{m} = (7L-2)N^2 \; , \tag{36}$$

since (29) requires only a complex matrix multiplication. The big disadvantage of the model (32) is that E_add and E_mult are usually unknown and therefore not specified in datasheets.

IV. Numerical Examples

Based on the adapted SIR (i.e., with channel estimation errors) and the energy model given in Section II-B, we numerically compare in this section different MIMO strategies with the energy consumption and the achievable SIR of a standard SISO system. This provides some insights into the trade-off between energy consumption and robustness and gives notes on the choice of appropriate transmit and receive strategies for different applications. To this end, we use typical sensor node hardware parameters (see Section IV-C) and channel matrices of maximum or minimum diversity order. The maximum diversity case is covered with probability one by using zero mean complex Gaussian channel matrices (i.e., non-line-of-sight (NLOS)) and the minimum diversity case by using a constant rank-one matrix (i.e., line-of-sight (LOS)), respectively.

A. Transmit and Receive Strategies

In this subsection, we shortly summarize the MIMO strategies that are used for comparisons with SISO.

1) Beamforming: The beamforming strategy refers to the case in which each link matches the transmit and receive beamformers to the own channel. Therefore, let $\boldsymbol{H}^{(k,k)} = \boldsymbol{V}^{(k,k)}\boldsymbol{\Sigma}^{(k,k)}\boldsymbol{U}^{(k,k)\mathsf{H}}$, $k \in \mathcal{K}$, with $\boldsymbol{\Sigma}^{(k,k)} \in \mathbb{R}_+^{N\times N}$ the diagonal matrix of singular values of $\boldsymbol{H}^{(k,k)}$ and $\boldsymbol{U}^{(k,k)}, \boldsymbol{V}^{(k,k)} \in \mathbb{C}^{N\times N}$ the unitary matrices of corresponding right and left singular vectors. Then, the column of $\boldsymbol{U}^{(k,k)}$ associated with the largest singular value is chosen as the transmit beamforming vector $\boldsymbol{u}_k \in \mathbb{C}^N$, $\|\boldsymbol{u}_k\|_2 = 1$, while the column of $\boldsymbol{V}^{(k,k)}$ associated to the largest singular value is defined to be the

$$V_{k\ell} = \frac{|h_{11}^{(k,k)*}h_{11}^{(k,\ell)} + h_{12}^{(k,\ell)*}h_{12}^{(k,k)} + h_{21}^{(k,k)*}h_{21}^{(k,\ell)} + h_{22}^{(k,\ell)*}h_{22}^{(k,k)}|^2}{2} + \frac{|h_{11}^{(k,k)*}h_{12}^{(k,\ell)} - h_{11}^{(k,\ell)*}h_{12}^{(k,k)} + h_{21}^{(k,k)*}h_{22}^{(k,\ell)} - h_{21}^{(k,\ell)*}h_{22}^{(k,k)}|^2}{2} \tag{40}$$

receive beamforming vector $\boldsymbol{v}_k \in \mathbb{C}^N$, $\|\boldsymbol{v}_k\|_2 = 1$. Thus the elements of the gain matrix $\boldsymbol{V}$ in (2) have the form

$$v_{k\ell} = \begin{cases} \frac{V_{k\ell}}{V_k} = \frac{|\boldsymbol{v}_k^{\mathsf{H}}\boldsymbol{H}^{(k,\ell)}\boldsymbol{u}_\ell|^2}{|\boldsymbol{v}_k^{\mathsf{H}}\boldsymbol{H}^{(k,k)}\boldsymbol{u}_k|^2}, & \text{for } k \neq \ell \\ 0, & \text{for } k = \ell \end{cases} \tag{37}$$

and the elements of the vector (4) of effective noise variances the form

$$z_k = \|\boldsymbol{v}_k\|_2^2 \frac{\tilde{\sigma}_k^2}{V_k} = \frac{\|\boldsymbol{v}_k\|_2^2 \tilde{\sigma}_k^2}{|\boldsymbol{v}_k^{\mathsf{H}}\boldsymbol{H}^{(k,k)}\boldsymbol{u}_k|^2} . \tag{38}$$

Remark 7. Choosing beamforming vectors only with respect to the own link is generally suboptimal in interference networks [14].

Beamforming requires channel knowledge at both sides of the link such that $\xi = 2$ in (13) and (14).

2) 2×2 Alamouti Space-Time Block Coding: For this strategy, all links in the network apply the Alamouti space-time block coding scheme from [15], such that the elements of the gain matrix can be expressed as

$$v_{k\ell} = \begin{cases} \frac{V_{k\ell}}{V_k} = \frac{V_{k\ell}}{\frac{1}{2}\|\boldsymbol{H}^{(k,k)}\|_F^2}, & \text{for } k \neq \ell \\ 0, & \text{for } k = \ell \end{cases} \tag{39}$$

with $V_{k\ell} \geq 0$, $k \neq \ell$, as in (40) at the top of the page [16], and the elements of the equivalent noise vector as

$$z_k = \frac{\tilde{\sigma}_k^2}{V_k} = \frac{\tilde{\sigma}_k^2}{\frac{1}{2}\|\boldsymbol{H}^{(k,k)}\|_F^2} . \tag{41}$$

Remark 8. Note that the SIR is equal for both Alamouti transmit symbols, which is generally not the case for higher order orthogonal space-time block codes [16].

In contrast to beamforming, Alamouti space-time block coding requires CSI at the receiver side only, so that we choose $\xi = 1$ in (13) and (14).

3) SISO Antenna Selection: For SISO antenna selection, the transmitter and receiver of each link form a SISO system by selecting the antenna elements that correspond to the best channel gain, that is $(i^\star, j^\star) = \arg\max_{1 \leq i,j \leq N} \big|h_{ij}^{(k,k)}\big|^2$, $k \in \mathcal{K}$. As in the case of beamforming, SISO antenna selection requires channel knowledge at both sides of the link.

B. Outage Probability

Besides considering the sum energy consumption required to achieve a certain SIR target, we consider in the simulations the outage probability as a function of γ, which is defined as

$$P_{\text{out}}(\gamma, \mathcal{P}) := \mathbb{P}\big(\boldsymbol{p}^\star(\gamma) \notin \mathcal{P}\big) \tag{42}$$

Here, the probability considers the outage events that either for a given SIR target no power allocation exists that guarantees $\forall k \in \mathcal{K} : \text{SIR}_k \geq \gamma$, or that a power allocation exists which however violates the power constraints. Simply put: given a transceive strategy, P_{out} visualizes with which probability a particular SIR target cannot be achieved.

TABLE II
SIMULATION PARAMETERS.

T_{F}	3 s	P_{mc}^{a}	3 mW
B	120 bytes	P_{mc}^{p}	15 μW
R	250 kbit/s	P_{tc}^{p}	35 μW
P	1 mW (0 dBm)	P_{tc}^{r}	35.5 mW
σ^2	-95 dBm	$P_{\text{in}}^{\text{ce}}$	31.3 mW
f_{MCLK}	8 MHz		

C. Simulation Parameters

For the numerical examples, we consider a multiantenna sensor network consisting of $K = 18$ interfering 2×2 links. Without loss of generality, each node is built of a bank of IEEE 802.15.4 compliant Chipcon CC2420 transceiver-chips [12], [17] (one for each antenna) and of a Texas Instruments MSP430F1611 microcontroller [18]. From the corresponding datasheets, we calculated the relevant simulation parameters summarized in Table II (considering the typical CC2420 supply voltage of 1.8 V), where the number B of payload bits per frame is chosen to generate in combination with T_{F} a low duty cycle, and where we set the noise variance on each receiver to the CC2420 receiver sensitivity (i.e., $\sigma_1^2 = \cdots = \sigma_K^2 = \sigma^2 = -95$ dBm).

According to the datasheet, the loss characteristic of the CC2420 between transmit powers and associated necessary input powers (see Section II-B) is slightly nonlinear but can be adequately approximated in the relevant transmit power range -25 dBm (3.162 μW)) - 0 dBm (1 mW) by the affine function

$$p_{\text{in},k} = f(p_k) = \alpha(p_k - 0.00316)\,\text{mW} + 15.3\,\text{mW} , \tag{43}$$

$k \in \mathcal{K}$, with $\alpha = (31.3 - 15.3)/(1 - 0.00316)$.

D. Evaluation

Since the performance of the strategies described in Section IV-A varies in dependency of the realization of the gain matrix $\boldsymbol{V}$, the numerical examples depicted in Figures 1–4 are based on 1500 independent channel realizations for each SIR target γ. In each run, $\boldsymbol{V}$ is randomly chosen and it is checked by the spectral radius $\rho(\boldsymbol{V})$ if γ is achievable (i.e., if $\rho(\boldsymbol{V}) < 1/\gamma$). If this is the case, the optimal transmit power allocation (6) is determined and subsequently the sum energy (12).

For each fixed γ, the corresponding sum energy consumptions may differ for different realizations of $\boldsymbol{V}$. However, the average over the 1500 sum energies is inadequate due

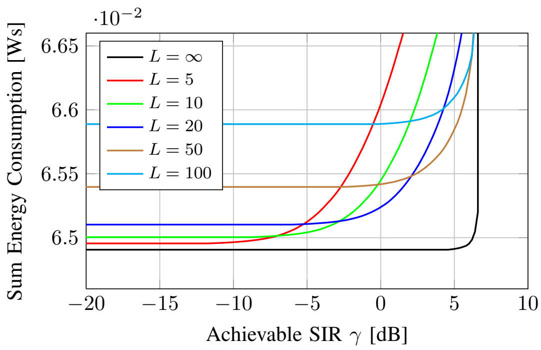

Fig. 1. Achievable SIR values per link vs. energy consumption per link for Alamouti space-time coding, different pilot sequence lengths L and a perfect NLOS channel. The scenario consists of $K = 18$ simultaneously active 2×2 links and the black line refers to the benchmark of perfect channel knowledge (i.e., $L = \infty$) without energy costs.

to the fact that divergent transmit powers can occur, which generate singularities (i.e., $p_k^\star(\gamma) \to +\infty$, for all $k \in \mathcal{K}$, if $\gamma \to 1/\rho(\boldsymbol{V})$). Therefore, the energy consumption plots in Figures 1–4 represent the 85^{th} percentile.

To illustrate the relative dependency of the trade-off between energy consumption and robustness on the length of pilot sequences for channel estimation, Fig. 1 depicts the sum energy consumption of Alamouti space-time block coding over achievable SIRs for different L and ideal NLOS channels. In this example, the maximum achievable SIR is approximately $6.8\,\text{dB}$ (i.e., $-10\log_{10}(\rho(\boldsymbol{V})) \approx 6.8\,\text{dB}$ in $85\,\%$ of all cases, resulting in a vertical energy slope). To achieve the same performance to within $0.4\,\text{dB}$ under channel estimation errors and $L = 100$, the energy consumption increases by $\approx 2.3\,\%$.

Figures 2 and 3 compare the strategies from Section IV-A for pilot sequence lengths of $L = 10$ and $L = 100$ and ideal NLOS channels. It turns out that SISO antenna selection achieves in this full-diversity scenario already for $L = 10$ a $\approx 10\,\text{dB}$ higher SIR than SISO at the cost of a negligible increase in energy consumption, while for $L = 100$, the energy consumption of SISO antenna selection compared to SISO is increased by $3.38\,\%$. In contrast, the maximum achievable SIR of Alamouti is that of SISO antenna selection at an approximately $75.5\,\%$ higher energy cost.

The significant difference in the basic energy consumption of Alamouti and Beamforming compared to SISO and SISO antenna selection relies on the fact that Alamouti and Beamforming use all transmit antennas. In contrast to Beamforming and SISO antenna selection, Alamouti and SISO do not require channel knowledge at the transmitter.[4]

It is clear that strategies that benefit from transmit and receive diversity are superior with respect to achievable SIRs in the ideal NLOS scenario. In the LOS situation depicted in Fig. 4, all strategies are therefore closer together such that in practice, switching between different strategies is favorable in dependency of the SIR requirements as well as of the current diversity order.

[4]SISO requires channel knowledge at the receiver to enable the coherent detection of symbols.

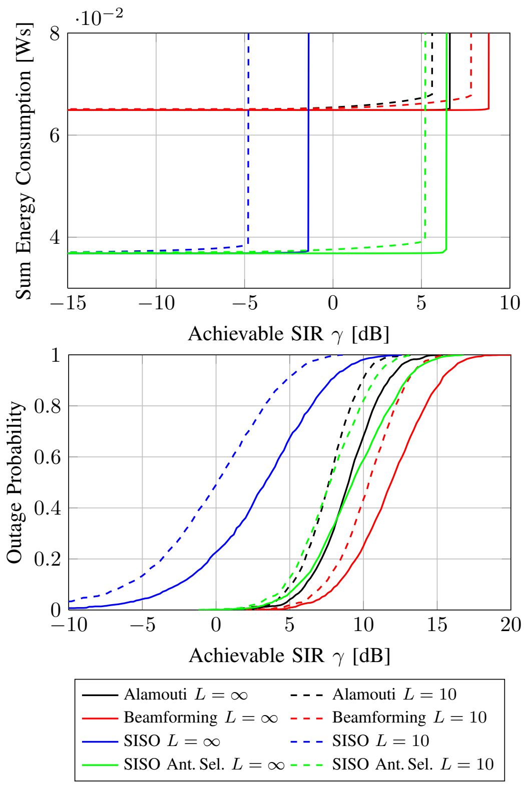

Fig. 2. Achievable SIR values vs. energy consumption and outage probability for pilot sequences of length $L = 10$ and perfect NLOS channels. The solid plots refer to the benchmark of perfect channel knowledge (i.e., $L = \infty$) without energy costs.

Remark 9. Compared to the basic energy consumption, the energy cost for channel estimation appears to be negligible in the depicted numerical examples. Note, however, that even an increase in energy consumption of $1 - 2\,\%$ can be crucial if network lifetimes of many years are required. In addition, due to Corollary 1, the energy consumption for channel estimation further increases if the number K of interfering links increases.

V. Conclusion

In this paper, the trade-off between energy consumption and robustness in power-controlled multiantenna sensor networks with interference was investigated. Since most multiantenna transmit and receive strategies are channel aware, after presenting a detailed energy model that takes into account circuit energy consumption, we analyzed the SIR degradation caused by channel estimation errors, to incorporate the trade-off between corresponding energy consumption and estimation accuracy. Then, based on the resulting adapted SIR model, we numerically compared different MIMO strategies with a standard SISO system for different pilot sequence lengths and different ideal channel models. It turns out that in an exemplary network of 18 interfering 2×2 full-diversity links, beamforming achieves up to $13\,\text{dB}$ higher SIR targets than SISO, at an increase in energy consumption of approximately $75\,\%$. On the other hand, a simple SISO antenna selection

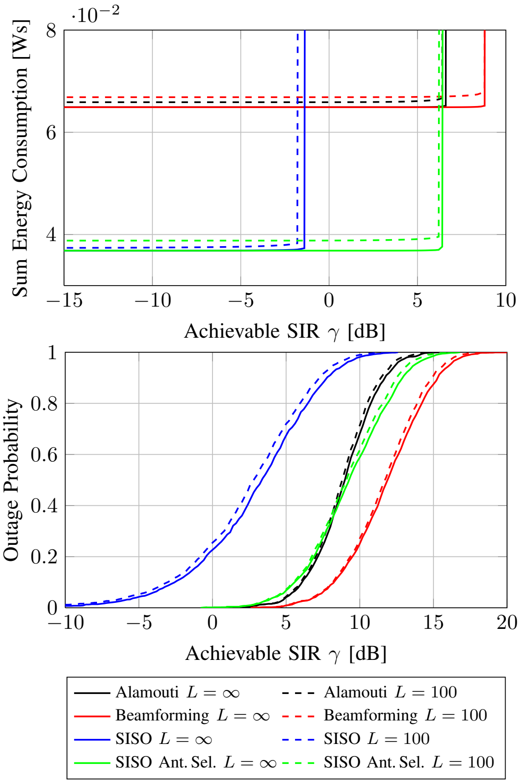

Fig. 3. Achievable SIR values vs. energy consumption and outage probability for pilot sequences of length $L = 100$ and perfect NLOS channels. The solid plots refer to the benchmark of perfect channel knowledge (i.e., $L = \infty$) without energy costs.

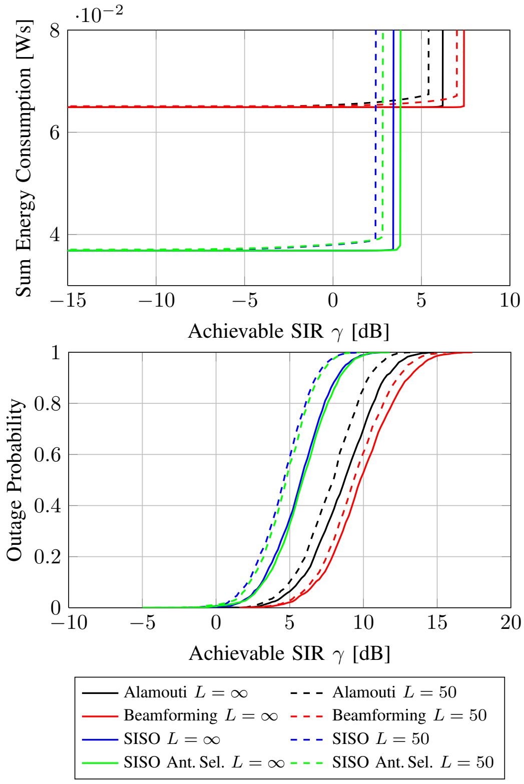

Fig. 4. Achievable SIR values vs. energy consumption and outage probability for pilot sequences of length $L = 50$ and perfect rank-one LOS channels. The solid plots refer to the benchmark of perfect channel knowledge (i.e., $L = \infty$) without energy costs.

strategy is able to achieve 10 dB higher SIRs than SISO by a negligible increase in energy consumption. Since this changes if the diversity order of the channels decrease, switching between different strategies is recommended.

Acknowledgment

The authors would like to thank Angela Feistel and Michał Kaliszan for helpful discussions.

References

[1] D. Tse and P. Viswanath, *Fundamentals of Wireless Communications*. Cambridge: Cambridge University Press, 2005.

[2] S. Cui, A. J. Goldsmith, and A. Bahai, "Energy-efficiency of MIMO and cooperative MIMO techniques in sensor networks," *IEEE J. Sel. Areas Commun.*, vol. 22, no. 6, pp. 1089–1098, Aug. 2004.

[3] Z. Chong and E. Jorswieck, "Energy-efficient power control for MIMO time-varying channels," in *Proc. IEEE Online Conference on Green Communications (GreenCom)*, New York, USA, Sep. 2011, pp. 92–97.

[4] A. Feistel, M. Wiczanowski, and S. Stańczak, "Optimization of energy consumption in wireless sensor networks," in *Proc. International ITG/IEEE Workshop on Smart Antennas (WSA)*, Vienna, Austria, Feb. 2007.

[5] M. Wiczanowski, A. Feistel, S. Stańczak, and H. Boche, "On energy cost of bit and bit/s in multi-antenna wireless networks under hardware constraints," in *Proc. International ITG/IEEE Workshop on Smart Antennas (WSA)*, Vienna, Austria, Feb. 2007.

[6] S. Stańczak, M. Wiczanowski, and H. Boche, *Fundamentals of Resource Allocation in Wireless Networks – Theory and Algorithms*, 2nd ed., ser. Foundations in Signal Processing, Communications and Networking. Berlin Heidelberg: Springer, 2009, vol. 3.

[7] W. Goh and K. Venkat, "MSP430 competitive benchmark," Texas Instruments Application Report (SLA205C), 2009.

[8] J. Polastre, R. Szewczyk, and D. Culler, "Telos: Enabling ultra-low power wireless research," in *Proc. 4th International Symposium on Information Processing in Sensor Networks (IPSN)*, Los Angeles, USA, Apr. 2005, pp. 364–369.

[9] S. M. Kay, *Fundamentals of Statistical Signal Processing: Estimation Theory*. Upper Saddle River, New Jersey: Prentice-Hall, 1993.

[10] H. Viswanathan and J. Balakrishnan, "Space–time signaling for high data rates in edge," *IEEE Trans. Signal Process.*, vol. 51, no. 6, pp. 1522–1533, Nov. 2002.

[11] T. F. Wong and B. Park, "Training sequence optimization in MIMO systems with colored interference," *IEEE Trans. Commun.*, vol. 52, no. 11, pp. 1939–1947, Nov. 2004.

[12] Texas Instruments, "MSP430x1xx family," User's Guide (SLAU049F), 2006.

[13] S. Yatawatta, A. P. Petropulu, and C. J. Graff, "Energy-efficient channel estimation in MIMO systems," *EURASIP Journal on Wireless Communications and Networking*, no. 2, pp. 1–11, Apr. 2006.

[14] S. Stańczak, M. Kaliszan, and M. Goldenbaum, "On distributed power control and transceiver optimization in wireless networks," in *Proc. 5th International ICST Conference on Performance Evaluation Methodologies and Tools (ValueTools)*, Cachan, France, May 2011.

[15] S. M. Alamouti, "A simple transmit diversity technique for wireless communications," *IEEE J. Sel. Areas Commun.*, vol. 16, no. 8, pp. 1451–1458, Oct. 1998.

[16] C. Schnurr, S. Stańczak, and A. Sezgin, "The impact of different MIMO strategies on the network-outage performance," in *Proc. International ITG/IEEE Workshop on Smart Antennas (WSA)*, Vienna, Austria, Feb. 2007.

[17] IEEE, "Standard 802.15.4 - 2003: Wireless medium access control (MAC) and physical layer (PHY) specifications for low rate wireless personal area networks (LR-WPANs)," 2003.

[18] Texas Instruments, "2.4 GHz IEEE 802.15.4 / zigbee-ready rf transceiver," Chipcon Products CC2420 Datasheet (SWRS041B), 2007.